MEMOIRS OF THE COLLEGE OF SCIENCE, University of Kyoto, Series A,
Vol. XXVIII, No. 2, Article 2, 1956

SEISMOMETRIC INVESTIGATION OF THE EARTH'S INTERIOR
PART III. ON THE STRUCTURE OF THE EARTH'S MANTLE (I)

BY

Yoshimichi KISHIMOTO

(*Received December 20, 1956*)

ABSTRACT

The structure of the earth's mantle, mainly its upper part, having been investigated by the analysis of seismic waves of five Kamchatka-Kurile Islands Earthquakes of shallow focus and some others, the problems on the existence and property of the 20°-discontinuity and the low-velocity layer in the mantle are discussed in some detail. The time-distance graphs is obtained in Japan are in fair agreement with Jeffreys-Bullen's Table (1939), and also the 20°-discontinuity is considered to exist certainly at nearly the same depth as given by Jeffreys. The amplitude relation observed at the epicentral distance near 20° between the direct wave propagating through the medium entirely above the 20°-discontinuity and the refracted wave penetrating down into that discontinuity is just the reverse of that commonly expected, that is, the former being small and the latter large both for the *P*- and *S*- waves. Concerning this phenomenon some arguments are given. Moreover, the existence of a new discontinuity was ascertained at some depth below the 20°-discontinuity, as deduced from the appearance of a prominent later phase. As to the existence of a low-velocity layer in the mantle, it is negatively concluded from the analysis of seismic waves observed at the stations in Japan of the earthquakes of Kamchatka-Kurile Islands, but the possibility of its existence near the crust in the form of pocket or reservoir is supposed to be not unreasonable, its problem being postponed to a succeeding paper.

1. Introduction

On the structures and properties of the earth's mantle, especially its upper part, many investigations have been carried out in various fields of research.

Seismometrically, many authors have published reports in this field, for example, H. Jeffreys (**1**, **2**, **3**, **4**, **5**), B. Gutenberg (**6**, **7**, 8), P. Byerly (**9**), I. Lehmann (**10**, **11**, **12**), and, in our country, H. Kawasumi (**13**, **14**), T. Matuzawa (**15**), and K. Wadati (**16**).

At present, one of the most important and interesting problems with regard to the structure of the earth's upper mantle as well as the crust may be relative to the two essentially different opinions for its construction. So far, most researchers including Jeffreys have held that the seismic wave velocities in the earth's mantle increase with depth and at the so-called 20°-discontinuity (its depth is estimated, for example, as 413 km below the earth's surface by Jeffreys) the rate of increase of velocity begins to rise abruptly. Jeffreys-Bullen's 1939 Table (**3**) is the most typical work of this opinion. On the other hand, in 1939 B. Gutenberg and C. F. Richter (**6**) initiated an entirely different opinion based on the observations of *P*-wave amplitude by using the North American earthquakes and observatories, that there exists a layer (so-called the low-velocity layer at present) in which the seismic wave velocities decrease with increasing depth, and which begins at about 80 km below the earth's surface. And they have further developed this opinion. According to Gutenberg's recent investigation (**8, 17**) it is said that the low-velocity layer exists in ranges between 60 km and 150 km for *P* and between 60 km and 250 km for *S*. And, moreover, he says that the 20°-discontinuity never exists at any depth.

I. Lehmann recently entertains a little different opinion (**11**). According to her, a low-velocity layer exists, but it is effective only for shear waves, and not for longitudinal waves and, moreover, far below this layer there exists also a discontinuity corresponding to the 20°-discontinuity at whose surface the change of seismic velocities is strong but gradual. Namely, her opinion is a compromise between the two opinions described above.

Of course, the velocity distributions of seismic waves are the most decisive data for the investigation of structure and properties in the earth's interior, so that the precise determination of velocity distribution is the most important, and the determination of velocity distribution is usually performed by the Herglotz-Wiechert method. But, in the application of this method, the data used have necessarily to belong to the same family of phase. If it is not so, the result of analysis is not correct. And whether a phase belongs to a certain family or not is never determined only by the precise reading of times of the first arrivals. For instance, according to Gutenberg, if there exists a low-velocity layer, only the diffracted waves arrive at as the *P*-phase in some ranges of epicentral distance and are read as the first *P*. If that is the case, the application of the Herglotz-Wiechert method will give rise to a faulty result.

To determine what family any phase belongs to is considered to be possible only with a detailed investigation of seismic wave development with distance extending over as wide ranges as possible. Namely, first, the following procedures are needed; 1) to take all later phases into consideration as well as the first arrivals of *P* and *S*. 2) to read the travel time, the amplitude, the period and as many other data as possible, and 3) to clarify the properties of each phase by taking all data obtained together into consideration. And by doing so, we shall be able to obtain many properties of each family of seismic waves and also to increase our information concerning the structures and properties of the earth's interior from various points of view.

Recently, this sort of investigation allowing for various observed data including the amplitude as well as the time-distance curve is increasing. Not to speak of

Gutenberg's investigation of the low-velocity layer, Lehmann's investigation above-cited (**11**) is also one in this course. And Bremaecker has recently published an investigation (**18**), in which he inferred the velocity distribution in the earth's mantle only by the observations of the amplitudes of the first *P*-waves between distance of 3° to 23°.

In the present investigation, several earthquakes which extended over areas of from about 6° to 26° were investigated in the course described above, and some interesting facts were found out, which will be described below in some detail.

2. Seismological data used in the analysis

For various reasons the seismological data used in the analysis are specially selected to fit the following conditions; 1) to use only the seismograms recorded with the seismographs of the same type, 2) to use as many observations as possible extending over the necessary distances, and 3) to use only the observations in nearly the same azimuth as seen from the epicenter. The first condition is convenient for the comparison and discussion on the amplitude and form of the seismic waves at each observatory, and the second condition may minimize the errors caused by the local character of each observatory founded on ground of different geological and crustal structure. The last condition will not approximately necessitate any consideration on the effect caused by the complex mechanism of earthquake occurrence at the hypocenter.

The Japan Meteorological Agency kindly permitted our copying of the seismograms recorded with the Wiechert Seismograph at 23 observatories attached to the Agency. By this courtesy the observations of epicentral distances extending over 6° to 26° were available for the present investigation. The constants of the Wiechert Seismograph used are as follows:

Component	Mass	Magnification	Period	Damping ratio
horizontal	200 kg	70～100	about 5 sec	5～10
vertical	80	50～ 80	,,	,,

The earthquakes examined were five Kamchatka-Kurile Islands earthquakes and some Formosa earthquakes. As the seismograms used in the analysis were obtained at the observatories in nearly the same azimuth seen from the epicenters of Kamchatka or Formosa earthquakes, the problem on the mechanism of earthquake occurrence is, in the present treatment, not taken into consideration. The positions of epicenters and the various data of those earthquakes are shown in Fig. 1 and Table 1 respectively. In this Table, the epicenters, focal depths and magnitudes are those after the United States Coast and Geodetic Survey (U.S.C.G.S.).

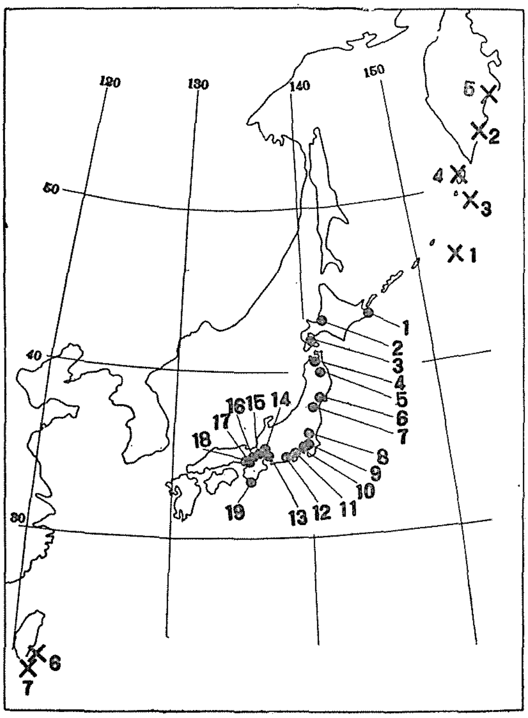

Fig. 1. Epicenters of earthquakes and observatories used in the present analysis. The cross and dot denote the epicenter and observatory respectively. Numbers of epicenter are referred to Table 1, and those of observatory are as follows: 1. Nemuro, 2. Sapporo, 3. Mori, 4. Aomori, 5. Morioka, 6. Sendai, 7. Fukushima, 8. Utsunomiya, 9. Tokyo, 10. Yokohama, 11. Mishima, 12. Shizuoka, 13. Nagoya, 14. Gifu, 15. Hikone, 16. Kyoto, 17. Osaka, 18. Kobe and 19. Shionomisaki.

Table 1. List of the earthquakes used in the present investigation. Latitude and longitude of epicenter, magnitude, focal depth and some of the origin time (*) are after the U.S.C.G.S.. The Greenwich Mean Time is adopted for the origin time.

No.	Date	Origin time (G.M.T.)	Epicentral region	Epicenter N E	Focal depth	Magnitude (Pasadena)	Observational range
		h m s		° °	km		
1	1952 June 22	21 43 02	SE off Shinshiru Is., Kurile Is.	46, $153\frac{1}{2}$	—	7	6°~17°
2	1952 Nov. 4	16 58 33	Near east coast of Kamchatka	$52\frac{1}{2}$, 159	—	$8\frac{1}{4}$	13°~25°
3	1953 Jan. 5	10 06 30	N part of Kurile Is.	49, 156	—	$6\frac{3}{4}$	9°~22°
4	1953 Oct. 11	13 08 34 (*)	"	50, $155\frac{1}{2}$	60	$6\frac{3}{4}$	10°~23°
5	1955 March 18	00 06 46	Near east coast of Kamchatka	$54\frac{1}{2}$, 161	—	—	19°~26°
6	1936 Aug. 22	06 51 37	Near SE coast of Formosa	22.1, 121.2	—	—	17°~24°
7	1955 Apr. 4	11 11 21 (*)	"	22, 121	—	6	17°~24°

3. Observational results

i) *Time-distance graph*

A typical example is the earthquake of January 5, 1953 (No. 3 in Table 1), which occurred at the northern part of the Kurile Islands, 49°N and 156°E. The observational data are given in Table 2, and some examples of the seismogram in Fig. 2 are given at the end of this article. Each value in Table 2 was read from the photographic copies of the original seismograms. The time-distance graphs of both *P* and *S* are shown in Fig. 3. In this figure, it is to be noted that both *P*- and *S*-graphs are divided into two branches intersecting at about 18°, and that the later branches are extended down to 13° in both *P*- and *S*-graphs, so that the graphs for the later phase up to 18° read after the first *P*- or *S*-phase are interpreted as the extention of the later branch observed beyond the distance of 18°. As will be described in the succeeding sections ii) and iii) and also as clearly seen from the seismograms in Fig. 2, these two phases are so clearly distinguished from one another by difference in their amplitudes and periods that there is no danger of confusing the two phases.

Focal depth of this earthquake is approximately estimated as 0.01 *R* according to Jeffreys' notation after *pP–S* duration at each observatory. Consequently the epicentral distance of about 18° which is the intersecting distance of our two branches stated above, will correspond to the so-called 20°-discontinuity referring to the Jeffreys-Bullen Table. In the J.-B. Table, two branches separated at the epicentral distance corresponding to the 20°-discontinuity are represented by two letters *d* and *r* respectively. The earlier branches at distances smaller than 20° are called *Pd* and *Sd*, and the later ones beyond 20° *Pr* and *Sr*. Namely, *Pd* and *Sd* represent the waves having their vertices above the 20°-discontinuity and

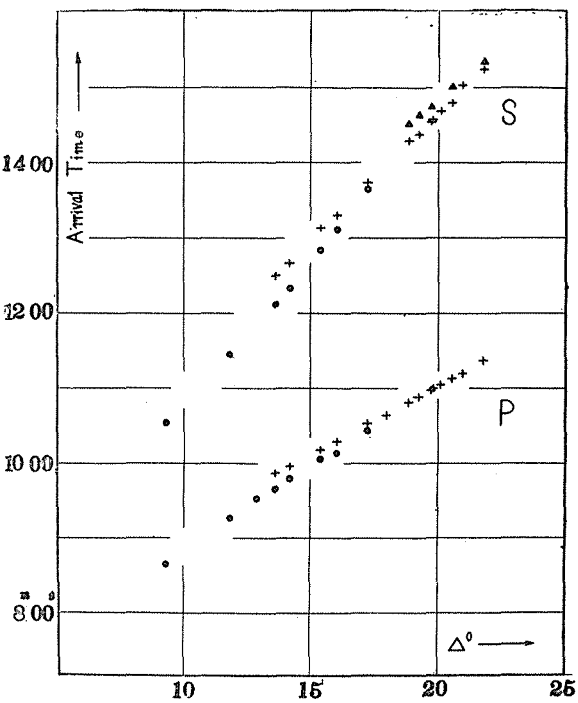

Fig. 3. Time-distance graphs of the earthquake of Jan. 5, 1953. Dots, crosses and triangles represent the *d*-wave (*Pd* and *Sd*), *r*-wave (*Pr* and Sr_1) and Sr_2-wave respectively.

Table 2. The earthquake of Jan. 5, 1953, 49°N, 156°E
0 : 10h06m30s.

Obervatory	Δ	Arrival time					O-C					Amplitude					Period				
		Pd	*Pr*	*Sd*	*Sr*$_1$	*Sr*$_2$	*Pd*	*Pr*	*Sd*	*Sr*$_1$	*Sr*$_2$	*Pd*	*Pr*	*Sd*	*Sr*$_1$	*Sr*$_2$	*Pd*	*Pr*	*Sd*	*Sr*$_1$	*Sr*$_2$
	°	m s	m s	m s	m s	m s	s	s	s	s	s	μ	μ	μ	μ	μ	s	s	s	s	s
Nemuro	9.32	8 39.4	—	10 32.2	—	—	− 4	—	+ 5	—	—	6.8	—	147	—	—	0.7	—	—	—	—
Sapporo	11.86	9 16.3	—	11 27.5	—	—	− 1	—	0	—	—	18.0	—	103	—	—	2.6	—	—	—	—
Mori	12.92	31.5	—	—	—	—	+ 1	—	—	—	—	11.5	—	—	—	—	3.7	—	—	—	—
Aomori	13.63	39.2	9 51.7	12 7.1	12 30.0	—	+ 1	+12	− 2	+20	—	8.5	21.0	260	540	—	2.7	—	1.0	4.7	—
Morioka	14.20	47.5	56.9	20.0	39.7	—	0	+10	− 9	+21	—	3.4	—	23	44	—	3.2	5.4	2.5	5.8	—
Sendai	15.41	10 3.1	10 10.5	50.2	13 7.8	—	0	+ 8	− 1	+17	—	5.4	22.4	50	181	—	1.9, 9.3	4.1	1.1	4.0	—
Fukushima	16.03	7.9	17.2	13 6.7	18.1	—	+ 1	+ 6	+ 1	+13	—	3.3	15.1	28	136	—	0.8, 5.2	4.1	1.2	3.6	—
Utsunomiya	17.25	26.1	31.3	38.5	44.0	—	0	+ 5	+ 6	+11	—	1.9	6.8	11	52	—	1.2	3.3	1.9	4.0	—
Tokyo	18.00	—	38.3	—	—	—	—	+ 4	—	—	—	—	4.3	—	—	—	—	—	—	—	—
Mishima	18.85	—	48.3	—	14 17.2	14 29.9	—	+ 4	—	+ 9	+22	—	4.8	—	28	158	—	4.2	—	5.1	4.4
Shizuoka	19.23	—	52.9	—	22.3	37.0	—	+ 4	—	+ 7	+22	—	7.2	—	—	112	—	3.9	—	5.6	4.9
Gifu	19.73	—	58.0	—	32.5	43.4	—	+ 4	—	+ 6	+17	—	23.3	—	57	145	—	4.1	—	5.7	—
Nagoya	19.82	—	59.6	—	33.9	—	—	+ 5	—	+ 6	—	—	21.3	—	54	153	—	3.8	—	—	4.5
Hikone	20.10	—	11 2.5	—	41.3	—	—	+ 5	—	+ 8	—	—	16.3	—	—	—	—	4.4	—	—	—
Kyoto	20.57	—	7.6	—	47.6	59.6	—	+ 5	—	+ 5	+17	—	14.9	—	20	64	—	4.3	—	—	—
Osaka	20.96	—	11.4	—	15 1.5	—	—	+ 5	—	+12	—	—	19.2	—	—	—	—	4.5	—	—	—
Shionomisaki	21.77	—	21.5	—	14.2	15 19.6	—	+ 7	—	+12	+17	—	21.3	—	13	97	—	4.1	—	5.8	5.0

Pr and *Sr* represent the refracted waves at the 20°-discontinuity. It is yet unknown whether two branches in our case intersecting at 18° correspond to Jeffreys' or not, but the same notation as Jeffreys' might tentatively be used for two branches in the present graph. Then, the fitness of the present time-distance graph to the J.-B. Table will be examined in the next step.

Recently, Jeffreys published (**4**, **5**) the revisions for his 1939 Table and stated the existence of regional differences in three areas, i.e. in Europe, Japan and North America. According to his revision, the 1939 Table is about right up to 17° but a reduction of 2 sec is needed beyond 22° for Japanese area. But, in the present treatment, the 1939

Table will tentatively be used. O–C in Table 2 shows the residual from the J.-B. 0.01 curve, taking $10^h 06^m 30^s$ as the origin time. These residuals were obtained in the following manner: Considering mainly the phase of *Pd* and moreover taking the other phases (*Pr*, *Sd* and *Sr*) for reference purposes, it was ascertained that the J.-B. 0.01 curve rightly fits for the present graph and the origin time was deduced as above mentioned. It is to be remarked that the J.-B. 0.005 curve calculated from the given 0.00 and 0.01 curves is practically most suitable for the present observed graph, but, in the present treatment, the difference of fitness for 0.005 and 0.01 curves is beyond our discrimination in respect to observational and analytical errors. If the focal depth is approximately assumed to be in the order of magnitude of $0.01R$ (R is the radius of the earth) the turning point of time-distance graph for the so-called 20°-discontinuity will be shifted to the epicentral distance of 18°, and it is well in accord with the present case. The *Pd*-branch fits best into the J.-B. 0.01 curve up to about 18°, and the fitness of the *Pr*-branch is comparatively good referring to its gradient although there are systematically positive residuals of a few seconds. The *Sd*-branch show some fluctuations, whose residuals, however, show minus signs at smaller distances and change their signs at larger distances, thus giving a little larger gradient than the J.-B. curve. But the *Sd*-branch is continuously traced up to 18° and no gap is observed on the time-distance graph. The *Sr*-branch roughly fits into the J.-B. curve referring to the gradient, but has systematically positive deviations in this case also.

The earthquake of November, 4, 1952 was one of the severest shocks and has been investigated in various research fields. The observational data are given in Table 3. This earthquake shows also the same tendency as that above-mentioned with regard to the development of seismic wave with distance. Namely, the time-distance graph of P-wave (as to S-wave, they were not accurately read due to scale-out in the seismograms or to extraordinarily large amplitudes) has two branches intersecting at about 18°. The residuals of both *Pd* and *Pr* from the J.-B. 0.01 curve, adopting the origin time, $16^h 58^m 33^s$, are given in Table 3. The fitness is fairly good not only for *Pd* but also for *Pr*, and the systematically plus residuals of *Pr* are not observed. On this point, the present earthquake differs from the previous one, which will be discussed in some detail in section 4.

Besides these two earthquakes, the following three were treated, their observing data being tabulated in Tables 4, 5 and 6 respectively. On the earthquake of June 23, 1952, only *Pd* and *Sd* were available owing to the smallness of the observing distance, and the fitness of P into the J.-B. 0.01 curve is fairly good. The earthquake of October 11, 1953 gave results similar to those of the two cases treated earlier. Lastly, the earthquake of March 18, 1955 also gave similar results, in which, however, only *Pr* and *Sr* were available owing to the largeness of observing distance. *Pr* and

Table 3. The earthquake of Nov. 4, 1952, 52½°N, 159°E
0 : $16^h58^m33^s$

Observatory	Δ	Arrival time		O-C		Amplitude		Period	
		Pd	*Pr*	*Pd*	*Pr*	*Pd*	*Pr*	*Pd*	*Pr*
	°	m s	m s	s	s	μ	μ	s	s
Nemuro	12.97	1 34.4	1 51.0	− 1	+16	11	14	0.9, 17.1	—
Urakawa	15.18	2 4.9	—	+ 1	—	12	—	1.1, 14.7	—
Sapporo	15.23	4.3	2 11.9	0	+ 8	13	22	—	—
Mori	16.33	18.5	24.5	0	+ 7	11	—	18.6	—
Aomori	17.18	27.5	33.0	− 1	+ 5	10	—	1.2, 15.7	—
Morioka	17.85	35.9	40.4	− 1	+ 4	—	19	—	4.0
Akita	18.35	43.1	47.1	+ 1	+ 5	—	14	—	6.3
Sendai	19.13	—	47.7	—	+ 2	—	—	—	5.1
Fukushima	19.75	—	59.5	—	+ 2	—	16	—	5.0
Utsunomiya	21.01	—	3 11.9	—	—	—	8	—	—
Nagoya	23.48	—	35.6	—	+ 1	—	16	—	5.8
Toyooka	24.22	—	45.0	—	+ 3	—	9	—	3.9
Shionomisaki	25.46	—	57.5	—	+ 6	—	—	—	—

Sr gave systematically plus residuals referring to the J.-B. 0.01 curve, in which the origin time was estimated as $00^h\ 06^m\ 46^s$ by comparing *Pr*-branch in this case with that of the earthquake of January 5, 1953. Since the positions of observatories are all nearly on a straight line seen from the epicenter of each earthquake in analysis, a small shift of epicenter will change their epicentral distances and azimuths slightly and to the same degree. Consequently, the gradient of the time-distance graph may be considered almost unchangeable and, moreover, a certain J.-B. curve to which each phase shows the best fit is kept also unchangeable by a small shift of epicenter.

Thus, from the results above-obtained, it may be concluded, at least from the standpoint of time-distance curve, that *Pd* and *Sd* correspond to the direct waves propagating through the material above the 20°-discontinuity and *Pr* and *Sr* are the refracted waves penetrating down into the 20°-discontinuity and again coming up to the earth's surface, both waves as being defined by Jeffreys in the J.-B. 1939 Table. In addition, the extending of *Pr*- and *Sr*-branches backward down to about 13° well coincides with what was discussed by Jeffreys in his 1939 paper (**3**). Therefore, it may safely be said that the existence of the 20°-discontinuity was ascertained by an analysis of the time-distance graph with regard to the data of earthquakes near Japan.

But, a question is left as to whether the 20°-discontinuity is of the first order or the second order. This question will be solved by finding a loop of the time-distance graph or the reflected wave at the discontinuity concerned. A P-phase was observed shortly after *Pr* on the seismograms of January 5, 1953, which forms a time-distance graph approximately similar to the upper branch of the loop or the reflection branch.

Table 4. The earthquake of June 22, 1952, 46°N, 153½°E
0 : $21^h43^m02^s$

Observatory	Δ	Arrival time		O–C	
		Pd	*Sd*	*Pd*	*Sd*
	°	m s	m s	s	s
Nemuro	6.36	43 34.0	44 48.7	− 1	+ 2
Sapporo	9.22	44 13.3	46 0.7	0	+ 5
Mori	10.17	27.4	22.1	+ 1	+ 3
Aomori	10.73	32.1	36.1	− 2	+ 3
Morioka	11.13	38.6	43.8	− 1	+ 2
Fukushima	12.84	45 3.3	47 29.6	+ 1	+ 7
Utsunomiya	14.04	18.3	—	+ 1	—
Tokyo	14.75	28.4	48 18.0	+ 2	+10
Yokohama	15.00	31.2	20.9	+ 1	+ 7
Mishima	15.62	39.4	35.2	+ 2	+ 7
Shizuoka	16.00	46.4	44.3	+ 4	+ 8
Nagoya	16.66	53.6	—	+ 3	—
Hikone	16.99	57.1	—	+ 2	—

Table 5. The earthquake of Oct. 11, 1953, 50°N, 155½°E
0 : $13^h08^m34^s$

Observatory	Δ	Arrival time		O–C		Amplitude		Period	
		Pd	*Pr*	*Pd*	*Pr*	*Pd*	*Pr*	*Pd*	*Pr*
	°	m s	m s	s	s	μ	μ	s	s
Nemuro	10.02	10 51.0	—	− 6	—	—	—	—	—
Sapporo	12.32	11 28.4	11 38.5	+ 1	+11	7.6	15.5	1.4	2.6
Mori	13.41	41.4	56.5	0	+15	5.2	18.7	3.3	3.5
Aomori	14.23	53.2	—	+ 1	—	3.2	—	—	—
Morioka	14.90	59.1	—	− 2	—	—	—	—	—
Sendai	16.18	12 18.7	12 22.5	+ 2	+ 6	2.8	8.2	—	6.0
Fukushima	16.79	23.4	30.2	− 1	+ 6	2.8	8.5	1.1	—
Utsunomiya	18.05	39.4	43.3	0	+ 5	0.2	6.9	—	3.6
Tokyo	18.83	—	—	—	—	—	2.7	—	—
Yokohama	19.09	—	54.1	—	+ 3	—	0.5	—	3.7
Mishima	19.65	—	58.5	—	+ 1	—	5.4	—	5.4
Shizuoka	20.03	—	13 4.3	—	+ 3	—	4.5	—	6.5
Nagoya	20.53	—	8.8	—	+ 3	—	6.5	—	4.6
Hikone	20.78	—	11.4	—	+ 3	—	3.8	—	4.2
Kyoto	21.23	—	17.3	—	+ 4	—	4.5	—	4.2

Table 6. The earthquake of March 18, 1955, $54\frac{1}{2}$°N, 161°E
0 : $00^h06^m46^s$

Observatouy	Δ	Arrival time			O—C			Amplitude			Period		
		Pr	Sr_1	Sr_2	*Pr*	Sr_1	Sr_2	*Pr*	Sr_1	Sr_2	*Pr*	Sr_1	Sr_2
	°	m s	m s	m s	s	s	s	μ	μ	μ	s	s	s
Aomori	19.35	11 10.4	14 42.5	14 56.0	+ 4	+ 8	+21	—	82	312	—	5.2	—
Morioka	20.05	16.3	51.8	15 8.1	+ 3	+ 3	+19	3.5	10	89	4.7	—	5.4
Sendai	21.35	30.4	15 20.7	28.2	+ 3	+ 7	+15	19.0	36	158	5.6	—	5.7
Fukushima	21.97	36.4	32.5	38.1	+ 3	+ 8	+14	11.3	41	92	5.0	5.3	6.4
Utsunomiya	23.24	49.5	—	56.8	+ 4	—	+10	10.6	—	50	4.4	—	4.1
Tokyo	24.03	58.4	—	—	+ 5	—	—	—	—	—	4.9	—	—
Yokohama	24.28	12 1.0	—	16 15.0	+ 5	—	+11	—	—	—	—	—	—
Mishima	24.86	7.1	—	23.7	+ 6	—	+10	12.8	—	42	4.9	—	4.8
Shizuoka	25.21	10.2	—	29.9	+ 6	—	+10	7.9	—	51	5.2	—	5.4
Gifu	25.57	12.0	—	35.0	+ 4	—	+ 9	5.1	—	12	5.2	—	5.2
Nagoya	25.68	12.8	—	—	+ 4	—	—	—	—	—	—	—	—
Hikone	25.91	15.8	—	37.1	+ 5	—	+ 6	5.7	—	10	5.0	—	—

But, its duration from *Pd* or *Pr* is much longer than that given in the J.–B. Table. Thus, in the present article, this problem must be left as unsolved, and will be investigated and reported in a succeeding paper.

ii) *Amplitude relation*

Concerning the phases *Pd* and *Sd* (both referred to as *d*–wave) and *Pr* and *Sr* (both referred to as *r*–wave), a clear and interesting fact is that the amplitude of *d*–wave becomes smaller and smaller with increasing distance, and the amplitude of *d*–wave is much smaller than that of *r*–wave near the distance of 18°. At the observatories of epicentral distance smaller than 13°, the seismograms are begun on the clear arrival of a *d*–wave and no *r*–wave is observed. At about 13° the arrival of a *r*–wave is first observed after the *d*–wave phase, and on the seismograms from 13° up to 18°, the *d*–wave of small amplitude is observed as the first motion, being followed by the *r*–wave of large swing as a later but clear phase. At the epicentral distance beyond 18° a *r*–wave of large amplitude first arrives and the following small *d*–wave cannot usually be identified, because it is disturbed by the wave train of the large *r*–wave of first arrival.

In Figs. 4, (a) and (b), some examples of amplitude-distance relation are given and the observed data are tabulated in the respective tables. The amplitude relation between *d*– and *r*–waves mentioned above is clearly observed on these graphs, in which the plotted points represent the amplitudes of horizontal movement owing to the lacking of vertical seismograms at many observatories, and moreover double amplitude is taken for the *S*–wave. In Fig. 5, the relation between the arrival time and observed amplitude for both *P*– and *S*–waves with respect to *d*– and *r*–waves are schematically shown which will afford a good guide for discussing the nature of this sort of phenomena.

This fact with regard to the amplitude relation of *d*– and *r*–waves is very interesting. Since, at the crustal discontinuity including the Mohorovičić discontinuity, this sort of phencmenon is never observed, the behaviour of seismic waves with relation to the 20°-discontinuity, if existing, has to be considerably different from that at the crustal discontinuity. Therefore, the amplitude relation above-mentioned is

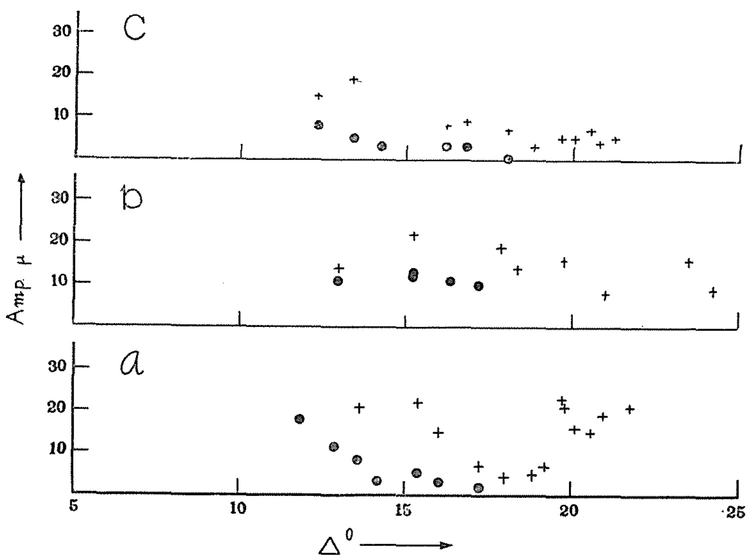

Fig. 4. a) Amplitude-distance graphs for *P*-wave. Notations have the same meanings as in Fig. 3.
a) The earthquake of Jan. 5, 1953
b) The earthquake of Nov. 4, 1952
c) The earthquake of Oct. 11, 1953

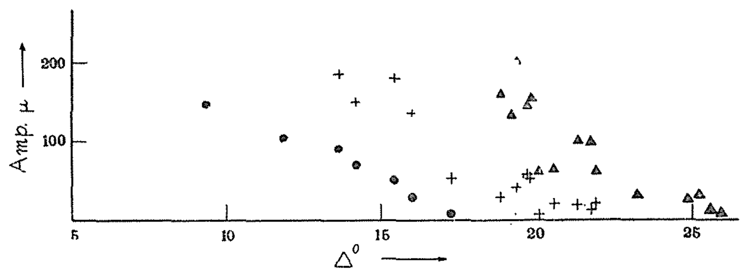

Fig. 4. b) Amplitude-distance graph for *S*-wave superposed of two earthquakes of Jan. 5, 1953 and March 18, 1955. in which the corrections are made for some observatories allowing for the local structural character. Notations have the same meanings as in Fig. 3.

considered to be an important key for the solution of the mantle structure, and will be discussed again in some detail in the later section **4**, i).

iii) *Wave period of each phase*

The periods of four phases, *Pd*, *Pr*, *Sd* and *Sr* of five earthquakes in Table 1 are plotted together in Fig. 6 with the period and epicentral distance as ordinate and abscissa respectively.

The *r*-wave periods are concentrated in a range of about 4 sec to 6 sec, independently of epicentral distance, observatory and earthquake. On the other hand, *d*-wave periods differ considerably. In some cases the very short period, and in other cases the fairly long period is prevailing, and, in addition, the superposition of the short period and the long one are sometimes observed. Roughly speaking, the periods of *d*-wave consist of periods shorter than about 2 sec and one longer than about 8 sec. Anyhow, it can safely be said without exception, at least in the earthquakes used in the present investigation, that *d*- and *r*-waves are clearly distinguished from each other alsofrom their differences in period. These data also possibly contribute to the investigation of the mode of propagation of both *d*- and *r*-waves and the properties of the mantle.

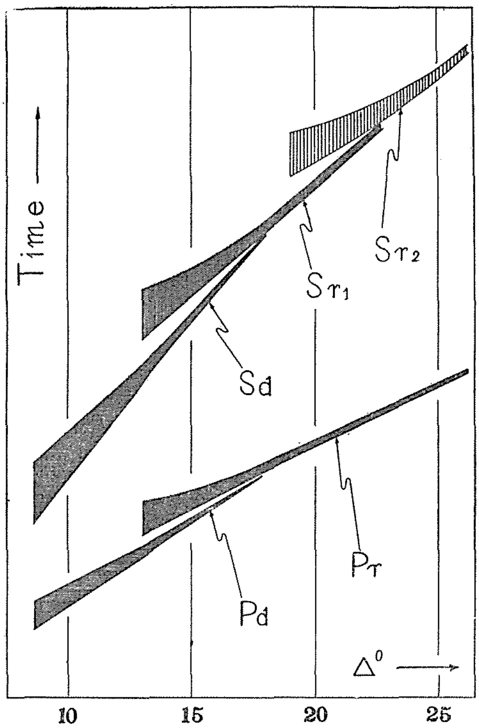

Fig. 5. Schematical illustration of the amplitude-distance relation. The breadth of each branch corresponds to the amplitude at the respective distances.

iv) *Sr_2-wave*

Concerning the earthquake of January 5, 1953, another fact is recognized. The *Sr*-wave amplitude described earlier decreases rapidly and a phase of large amplitude is observed after *Sr* beyond about 19°, and the duration between *Sr* and this phase becomes shorter and shorter with increasing distance. These aspects are clearly seen in Figs. 3 and 5. Thus, this phase seems to belong to a new branch different from that of the *Sr*-wave, and hereafter this phase and the previous *Sr* will be called Sr_2 and Sr_1 respectively. The time-distance graph of Sr_2 is nearly a straight line, whose apparent velocity is 6.4 km/sec. From the diminishing of duration between Sr_1 and

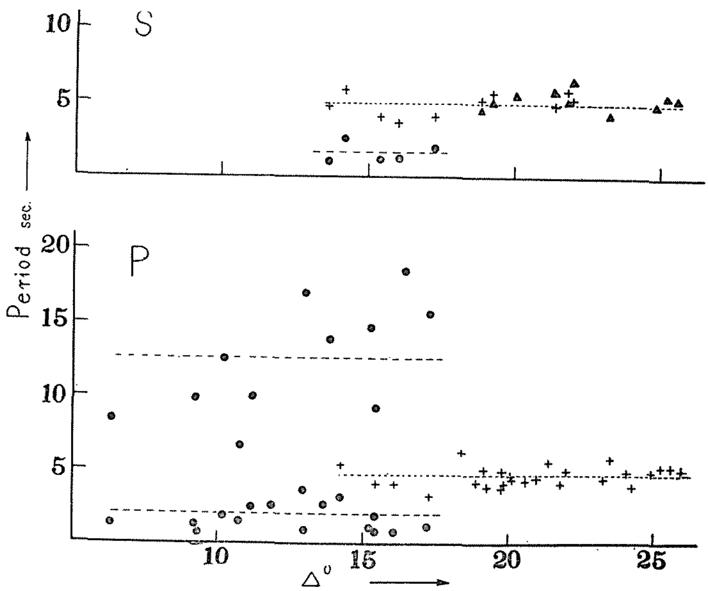

Fig. 6. Period-distance relation of each phase. Notations have the same meanings as in Fig. 3.

Sr_2 with increasing distance, these two branches are finally to intersect at a certain distance, but unfortunately, we have no observation beyond 22° as to this earthquake, so that we are obliged to examine this problem by an earthquake presenting more data.

The earthquake of March 18, 1955, mentioned above in §**3**, i), is suitable for the present purpose, because this earthquake has the observational data from about 19° up to 26°. Some seismograms are shown in Fig. 7. In this case also, the time-distance graph of S-curve is divided into two branches which intersect at about 24°, and the apparent velocities of these two branches are 5.4 km/sec and 6.6 km/sec respectively. These numerals, 5.4 km/sec and 6.6 km/sec, coincide very well with those of the earthquake of January 5, 1953. The residuals of Sr_1 and Sr_2 from the J.-B. 0.01 curve are tabulated in Table 6 in the previous section i). In Fig. 8, the travel-time graphs of these two earthquakes are shown, calculated from the respective origin times. In this figure, it is clearly recognized that the behaviours of S-waves of both earthquakes are in a fairly good agreement. Moreover, in most seismograms, as seen in Fig. 7, the commencement of Sr_2 is so clear that we can easily identify the appearance of Sr_2-wave. And the amplitude-distance relations of Sr_1 and Sr_2 are nearly the same in both earthquakes as seen in Fig. 4, b).

Thus, from the data above-mentioned, it is roughly concluded that there may be a discontinuous plane at some depth below the 20°-discontinuity, namely that Sr_2 at distance smaller than about 24° is the backward extension of the branch beyond 24°. Concerning this problem, it can be stated that at about 24° the J.-B. 0.01 curve shows a clear change, though gradual, of its gradient.

It is to be noted that this result was deduced only from the analysis of the S-wave, and as to the P-wave no later phase was observed at the distances concerned. Although the amplitudes of the first P shows a maximum near the critical distance, say about 24° and it seems that there exists a change of wave-form suggesting the superposition of two waves near the critical distance, these are less reliable than those of the S-wave. Consequently, this new discontinuity, if existing, is considered to be more effective for S than P. Needless to say, this problem on new discontinuity should be discussed by much more abundant and more accurate data, but the above-observed fact is considered to be useful for a new development of the investigation of the earth's mantle.

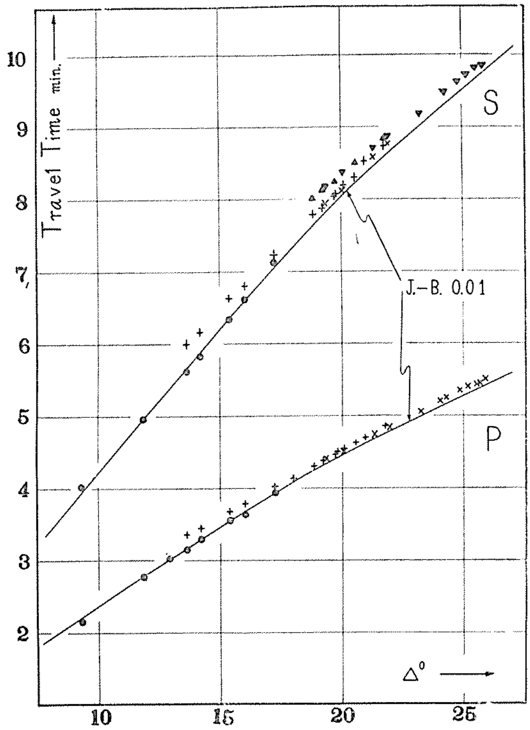

Fig. 8. Travel time-distance graphs superposed of two earthquakes of Jan. 5, 1953 and March 18, 1955. ●, + and ▲ belong to the former, and × and ▼ represent the r-wave and Sr_2-wave for the latter respectively.

In connection with the newly proposed discontinuity, Nishitake (**19**) recently discussed the property of the earth's mantle and obtained the distribution of k/μ (k and μ are the bulk modulus and rigidity respectively) with depth as deduced from the J.-B.'s seismic velocity distribution. In his paper it was reported that an abrupt decrease takes place at about 100 km below the 20°discontinuity and this decrease keeps on for about 100 km. The decrease of k/μ corresponds to the larger increase of μ compared with that of k with increasing depth, and this behaviour of k/μ seems to relate possibly to the present new discontinuity.

4. Some considerations

i) *On the amplitudes of d– and r–waves*

Gutenberg previously stated (7) that the amplitude of the first *P*–wave shows an abrupt decrease at about 5° and is very small at distances up to about 15°, and beyond 15° becomes gradually large with increasing distance. And he attributed the cause of these phenomena to the existence of a low-velocity layer in the mantle, namely, the waves of small amplitude at 5° to 15° are the diffracted waves due to that low-velocity layer and the large waves observed beyond 15° are the wave penetrating down into this low-velocity layer and again rising up to the earth's surface. According to his recent paper (8), this diffracted wave of the normal earthquake composes a nearly straight time-distance curve whose apparent velocity is 7.74 km/sec and deviates considerably from the the J.–B. curve. On the other hand, as to the *S*–wave, it is said that there is no observation in the range of about 10°∼17°.

In any case, since the amplitude variation with distance stated by Gutenberg seems to be similar in some points to the facts described in §3, ii), a consideration on Gutenberg's structure is to be made. The conception of 'low-velocity layer' by Gutenberg is assumed on the basis of the following two phenomena; namely, 1) the sudden diminution of amplitude at about 5° and its continuation up to about 15°, and 2) the gradual and monotonous increase of amplitude from about 15° up to beyond 20°. Accordingly, these two points should be examined regarding the earthquakes concerned here. In order to examine the first relation, the amplitude-distance relations of the first *P*–motion of three earthquakes at short distances near 5° were investigated, whose results are illustrated in Figs. 9, a), b) and c). Of these earthquakes, the first was the Akita-Oga Earthquake on May 1, 1939 whose focal depth was considered to be shallower than 10 km. The second was the earthquake of July 28, 1951 whose epicenter and focal depth were estimated as 37.5°N, 143.5°E and about 10 km respectively, and the third was the Yoshino Earthquake of July 17, 1952 whose focal

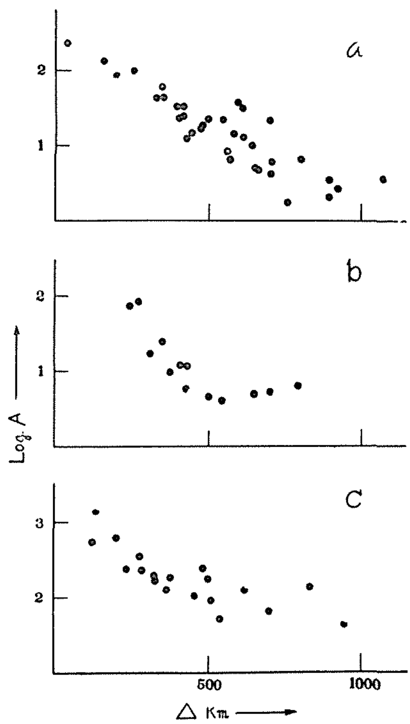

Fig. 9. Amplitude-distance graphs for the first *P*–motion at short distances. a) The Akita-Oga Earthquake of May 1, 1939, b) The earthquake of July 28, 1951, and c) The Yoshino Earthquake of July 17, 1952.

depth was estimated as 70 km below the earth's surface and this depth corresponds to the top of low-velolocity layer, if it exists. In Fig. 10, the natural logarithm of amplitude is plotted against the epicentral distance. In any case, the sudden diminution of amplitude at about 5° as assumed by Gutenberg was not observed. Next, for the second relation, as was already described, the *d*–waves are observed equally on both *P*– and *S*–waves, and continue with no gap up to about 18° at which the *d*–waves are overtaken by the *r*–waves, and, moreover, the amplitudes of *d*–wave decrease monotonously up to 18° and never increase again. In addition, the time-distance graphs of *d*–waves fit fairly well into the J.–B. Table from about 6° to 18° as was mentioned in the previous §**3**, i). Considering these results, it is reasonably concluded that the present case differs certainly from that of Gutenberg, and so the existence of a low-velocity layer in the mantle is considered questionable at least in the case of Japanese earthquakes.

According to the recent investigations of Jeffreys cited in the previous §**3**, i) (**4**, **5**), there exist considerable regional differences between the time-distance curves in European, Japanese and North American regions, and these differences imply the regional difference of the mantle structure down to considerable depth. On the other hand, Lehmann (**11**, **12**) also found that the time-distance graphs of the *S*–wave give the different aspects in Europe and North America. Reflecting upon these facts, the allowance for the regional difference may be possibly assumed in the present investigation.

In any way, however, the phenomena mentioned above in §**3**, ii) concerning the amplitudes of *d*– and *r*–waves will be interpreted as caused by an abnormally strong attenuation of *d*–waves observed near the epicentral distance of 18° or by an abnormal enlargement of *r*–waves owing to some causes. In order to examine this point, a deep earthquake was treated for reference. This earthquake occurred on February 28, 1950 and its epicenter and focal depth were 46.0°N, and 143.8°E, and 350 km respectively, and so this earthquake is considered to have been seated above the 20°–discontinuity but below the low-velocity layer, if existent. In Fig. 10, the amplitude of the first *P* arrival is plotted against the epicentral distance. Since this earthquake was a very large one and the onsets of the first *P* arrival was very clear, there is no doubt with regard to the readings of amplitude.

In this figure, the amplitudes are small in some ranges before about 12°, and increase abruptly at about 12° which may nearly correspond, allowing for the focal depth, to the amplitude relation which should be observed near the epicentral distance of 20° in the case of shallow earthquakes. Thus the deep earthquake, if its focus is above the 20°–discontinuity, shows the same behaviour with regard to the anomalous diminution of amplitude at an epicentral distance at which *Pr*–wave is expected to appear first.

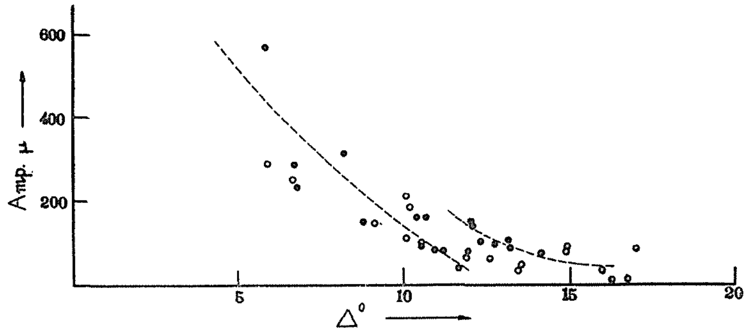

Fig. 10. Amplitude-distance graph for the first P-motion of the deep earthquake (350 km) of Feb. 28, 1950.

Then, the reasonable interpretation of the behaviours of amplitude of both d- and r-waves is fairly difficult. One probable interpretation is the diminution of the d-wave due to the existence of a transient layer just above the 20°-discontinuity which makes the amplitudes of both P and S diminish equally. On the other hand, the enlargement of the r-wave may possibly be considered as reflecting the constancy of r-wave period and the possible existence of another discontinuity below the 20°-discontinuity as mentionedin § **3**, iv). The emphasis on a specified period of the critically refracted wave in the case of a layer overlying a semi-infinite medium was worked out by Sato (**20**) and Officer (**21**). These investigations seem to be worthy of examination in the present case, although it is problematical whether or not these are valid for a layer in the earth's interior.

Finally, some remarks are conveniently added in this occasion. As was mentioned in § **3**, i), Pr- and Sr-waves showed positive residuals of a few seconds compared with the J.-B. curve for some earthquakes, but this is not the case for others. This phenomenon may be related with the magnitude of earthquake and with the sensitivity of seismograph. On the earthquake of November 4, 1952, the P-wave of clear onset beyond about 18° was forerun by a weak vibration which fitted into the J.-B. curve. On the earthquake of October 11, 1953, the Galitzin-type seismograph of high magnification (about 2000) at the Kamigamo Geophysical Observatory, Kyoto University, showed a similar weak vibration forerunning Pr of clear onset. On these two earthquakes, the weak vibration fits into the J.-B. curve and the following wave of clear onset (Pr) is delayed by a few seconds. Other earthquakes show only a Pr-wave of clear onset, missing the weak vibration. These facts may be justified by the explanation that the weak vibration is missed by refraction at the 20°-discontinuity in some cases.

ii) *On the Formosa earthquakes*

As the comparison of northern earthquakes seen from Japan (Kamchatka-Kurile

Table 7. The earthquake of Aug. 22, 1936, 22.1°N, 121.°2E
0 : 06h51m37s

Observatory	Δ	Arrival time			O—C			Period of Pr
		Pd	*Pr*	*S*	*Pd*	*Pr*	*S*	
	°	m s	m s	m s	s	s	s	s
Kobe	17.44	55 37.0	55 45.4	59 11.4	− 2	+ 6	+21	3.7
Kyoto	18.00	46.8	51.0	19.9	+ 1	+ 5	+17	3.7
Nagoya	18.87	57.4	56 00.2	34.5	+ 1	+ 3	+12	3.3
Gifu	18.89	55.8	00.1	32.0	− 1	+ 3	+ 9	3.4
Mishima	20.13	—	11.4	58.5	—	+ 1	+ 8	5.0
Nagano	20.59	—	15.4	00 6.7	—	0	+ 8	3.6
Tokyo	21.01	—	21.6	—	—	+ 2	—	6.5
Kumagaya	21.02	—	20.5	19.3	—	0	+12	6.0
Fukushima	22.69	—	36.7	42.1	—	0	+ 4	3.5
Sendai	23.27	—	41.0	50.8	—	− 1	+ 2	3.4
Morioka	24.34	—	51.0	01 12.5	—	− 2	+ 5	5.5

Islands) with southern earthquakes, two Formosa earthquakes, mainly that of August 22, 1936, were likewise analysed with regard to the travel-time, amplitude and period of each phase. The earthquake of August 22, 1936 is considered to be very shallow-seated in the crust, because this earthquake did some damages to the buildings near its epicenter. The observational data are given in Table 7 and some examples of seismogram in Fig. 12. The time-distance graphs of both *P* and *S* are shown in Fig. 11, in which, unfortunately, the seismograms at distance smaller than about 17° were not available. As shown in Fig. 11, the abrupt change of gradient is clearly observed at about 20° as to the time-distance graph of *P*-wave. This value

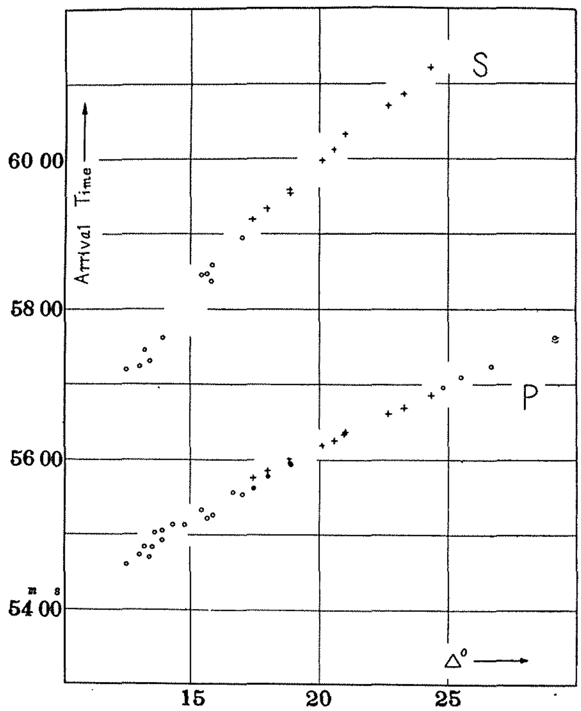

Fig. 11. Time-distance graphs of the Formosa earthquake of Aug. 22, 1936. Circles are the readings after the Japan Meteorological Agency added for reference, and other notations are referred to Fig. 3.

of 20° is well accordant with the so-called 20°-discontinuity as observed in shallow earthquake, and clearly shows the existence of a 20°-discontinuity in the Japanese area.

The first *P* waves at distances up to about 20° are weak and their periods are short, and moreover, they are followed by waves of clear onset and long period. On the other hand, beyond 20°, the seismograms are commenced by a wave of clear onset which corresponds to the latter *P*-wave at distances up to about 20°. This change of the appearance of the first *P* arrival with increasing distance is the same as that of the Kamchatka earthquake; accordingly, we may call them *Pd* and *Pr* respectively. *Pd*-waves up to about 20° fit fairly well into the J.-B. 0.00 curve, as seen in Table 7, allowing for the first *P* arrivals from 2° to 7° in Formosa observatories which are considered the *Pd*-waves. And, moreover, *Pr*-waves beyond 20° approximately fit to the same curve. But, there exists a slight difference between the Formosa and the Kamchatka earthquakes. In the latter case, *Pr*-branch beyond 18° (corresponding to 20° in the Formosa earthquake) was extended back almost linearly down to about 13°, but in the former, two *Pr*-branches, say, one up to 20° and the other beyond 20°, have the different slopes and intersect at about 20°, as seen in Fig. 11. Therefore, judging only from this fact alone, it is naturally to consider that there exist two branches belonging to different families, and this consideration is suggested by another phenomenon, namely, the period of *Pr* which is about 3.5 sec up to about 20°, becoming 6.0 sec at 21°, and thereafter returning to about 3.5 sec. Recently, Z. Suzuki (**22**) stated that a similar phenomenon was observed at the superposition of direct and refracted waves at the so-called critical distance on the small scale explosion experiment. If a similar explanation is valid in the present case of natural earthquakes, it results that three branches, say, *Pd* and two *Pr*'s, meet at about 20°. In the present state, however, it is impossible to accurately determine as to whether there exists a difference between the observed materials of both the Kamchatka- and Formosa-earthquakes, because the observed materials of Formosa earthquakes are far inferior to those of Kamchatka-Kurile Islands in the points of example-number and distribution of observatories.

Next, concerning the *S*-wave, the arrival time observed of the *S*-phases observed after the distance of 20° is approximately accordant with the J.-B. 0.00 Table, but the *S*-phase clearly observed before the 20° is considered to be the *Sr*-wave and not the *Sd*-wave, as shown in Fig. 12 and Table 7. Contrary to the case of Kamchatka-Kurile Islands, it is difficult to find the *Sd*-wave preceding the *Sr*-wave in a distance shorter than 20°. And moreover, in case of Formosa earthquake, the available observatories are lacking between 2°- and 17°-epicentral distance. Under such disadvantageous circumstances the discussion of the comparison between the earthquakes of northern and southern origin seen from Japan is inappropriate in the present state, but the minute regional difference of the mantle structure, if existing, will be discussed in greater detail in a succeeding paper.

iii) *On the* 13°*-discontinuity*

In 1951, the writer (**23**) reported that an abrupt change was observed at about 13° of the gradient of superposed time-distance graph of about ten shallow earthquakes having occurred in the same epicentral region of Japan and having nearly equal focal depths, and he provisionally called it a 13°-discontinuity. It was left unexplained, however, as to whether it corresponded to a real discontinuity or was only an apparent phenomenon

Now, reflecting upon the facts described in this article and allowing for the apparent velocity, 9.5 km/sec, of the branch at range between 13° and 20° in our article above-cited, it may naturally be inferred that the abrupt change of gradient of superposed time-distance graph at 13° is caused by missing of *Pd* owing to its weakness and misreading of *Pr* as the first motion at many observatories. And, moreover, a considerably large fluctuation of the observed *P*-time at distances near 13° may possibly support the interpretation above-mentioned. And moreover, the epicentral distance of 13° is estimated to be the shortest distance at which the *Pr*-wave is expected to be clearly observed. Consequently the anomalous appearance in the time-distance graph whihc was previously reported as the 13°-discontinuity is, after all, reasonably explained by the refracted waves connected with the existence of 20°-discontinuity in the earth's mantle.

5. Summary

Seismograms observed at observatories in Japan of five prominent earthquakes of Kamchatka-Kurile Islands were analysed to investigate the existence and nature of the 20°-discontinuity and the low-velocity layer in the earth's mantle. Some results obtained in the present treatment are as follows:

i) The existence of the 20°-discontinuity was ascertained in Japan, but its order of discontinuity remains undetermined.

ii) The existence of low-velocity layer was negatively concluded, at least in Japan.

iii) The abnormal diminution of amplitude of direct seismic wave and, reversely, the large and clear appearance of a refracted seismic wave through the 20°-discontinuity were definitely observed for both *P*- and *S*-phases near the epicentral distance of 20°. For these remarkable facts two explanations of the large attenuation of direct wave at the transition layer close above the 20°-discontinuity or any enlargement-effect for the refracted wave by the

layer-channel between the 20°-discontinuity and the 25°-discontinuity newly found, were tentatively postulated.

iv) From the present treatment, it is reasonably concluded that the nature and structure of the earth's mantle may have somewhat regional character when they are compared for the regions in Europe, America, Asia, etc.

Acknowledgement

The writer wishes to express his hearty gratitude to Prof. E. Nishimura for his kind guidance throughout the present investigation, and also to the directors and members of the Japan Meteorological Agency for their generous permission for copying many seismograms. The cost for the present study was partly defrayed by a grant-in-aid for Scientific researches of the Ministry of Education.

REFERENCES

1. H. JEFFREYS, The structure of the Farth down to the 20°-discontinuity, Mon. Not. Roy. Astr. Soc., Geophys. Suppl., **3** (1936), 401-422.
2. ——————, —————————————————— (second paper), Mon. Not. Roy. Astr. Soc., Geophys. Suppl., **4** (1936), 13-43.
3. ——————, The times of *P*, *S* and *SKS*, and the velocities of *P* and *S*, Mon. Not. Roy. Astr. Soc., Geophys. Suppl., **4** (1939), 498-533.
4. ——————, The times of *P* up to 30°, Mon. Not. Roy. Astr. Soc., Geophys. Suppl., **6** (1952), 348-364.
5. ——————, The times of *P* in Japanese and European earthquakes, Mon. Not. Roy. Astr. Soc., Geophys. Suppl., **6** (1954), 557-565.
6. B. GUTENBERG and C. F. RICHTER, New evidence for a change in physical conditions at depths near 100 km, Bull. Seism. Soc. America, **29** (1939), 531-537.
7. B. GUTENBERG, On the layer of relatively low wave velocity at a depth of about 80 kilometers, Bull. Seism. Soc. America, **38** (1948), 121-148.
8. ——————, Low-velocity layers in the earth's mantle, Bull. Geol. Soc. America, **65** (1954), 337-348.
9. P. BYERLY, The Montana earthquake of June 28, 1925, Bull Seism. Soc. America., **16** (1926), 209-265.
10. I. LEHMANN, Transmission times for seismic waves for epicentral distances around 20°, Geod. Inst. Kobenhavn, Med., **5** (1934), 1-46.
11. ——————, *P* and *S* at distances smaller than 25°, Trans. Amer. Geophys. Union, **34** (1953), 477-483.
12. ——————, *The times of P and S in Northern America*, Estratto da Annali di Geofisica, 8 (1955), 351-370.
13. H. KAWASUMI and S. HONMA, On a problem concerning the internal structure of the earth as discussed from the time-distance curve of the Formosa Earthquake of April 20, 1935, Bull. Earthq. Res. Inst., **14** (1936), 201-221.
14. H. KAWASUMI, Study on the propagation of seismic waves (the first paper), Bull. Earthq. Res. Inst., **10** (1932), 94-119.
15. T. MATUZAWA, Seismometrische Untersuchungen des Erdbebens von 2, März 1933, I. Bestimmung des Herdes, Bull. Earthq. Res. Inst., **13** (1935), 171-193.

16. K. WADATI and K. MASUDA, On the travel time of earthquake waves (Part V), Geophys. Mag. **7** (1933), 269–290.
17. B. GUTENBERG, Wave velocities at depths between 50 and 600 kilometers, Bull. Seism. Soc. America, **43** (1953), 223–232.
18. J. CL. DE BREMAECKER, Use of amplitudes, Part I: Pn from 3° to 23°, Bull. Seism. Soc. America, **45** (1955), 219–244.
19. T. NISHITAKE, Elastic properties of rocks with relation to the earth's interior, Mem. Coll. Science, Kyoto Univ., A, **28** (1956). 73–98.
20. Y. SATO, Study on surface waves, VI Generation of Love and other types of SH waves, Bull. Earthq. Res. Inst., **30** (1952), 101–120.
21. C. B. OFFICER, Jr., The refraction arrival in water covered areas, Geophysics, **18** (1953), 805–819.
22. Z. SUZUKI, On the forms of seismic wave generated by the explosion (3rd paper), Bull. Research Group of Seismic Exploration, **7** (1956), 43–59 (in Japanese).
23. Y. KISHIMOTO, On a 13°-discontinuity of the earth's mantle, Zisin, 2nd Ser., **5** (1951), 7–12 (in Japanese).

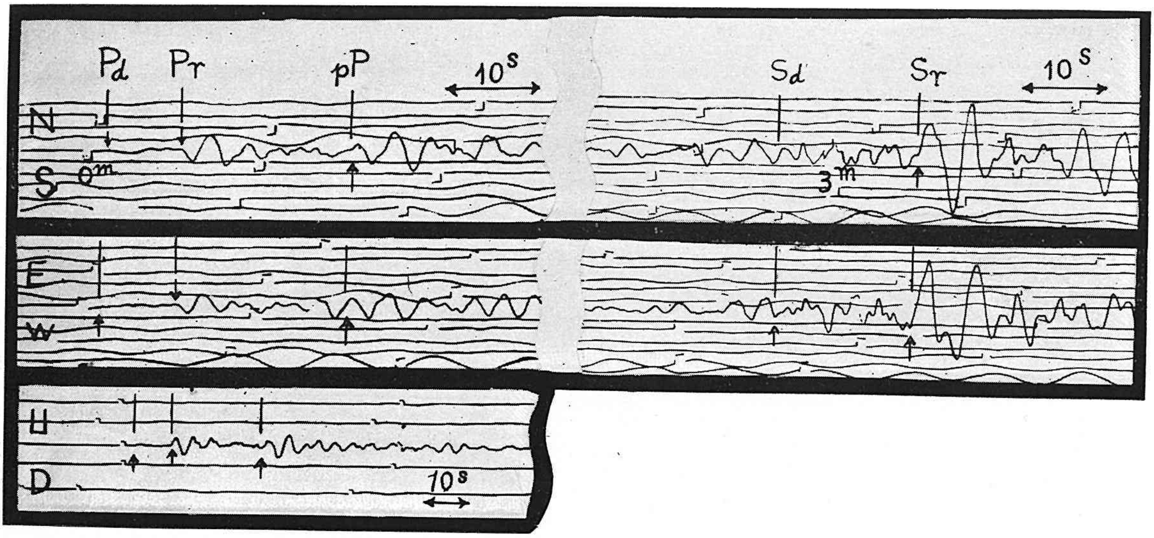

Fig. 2. Wiechert-seismograms, Jan. 5th 10h 06m 30s, N Part of Kurile Islands (referred to Table 2)
(a) Sendai (Δ=15.41°) The weak *Pd* and *Sd* appear as the first motion, being followed by *Pr* and *Sr* of large swing.
(By the courtesy of the Sendai Observatory)

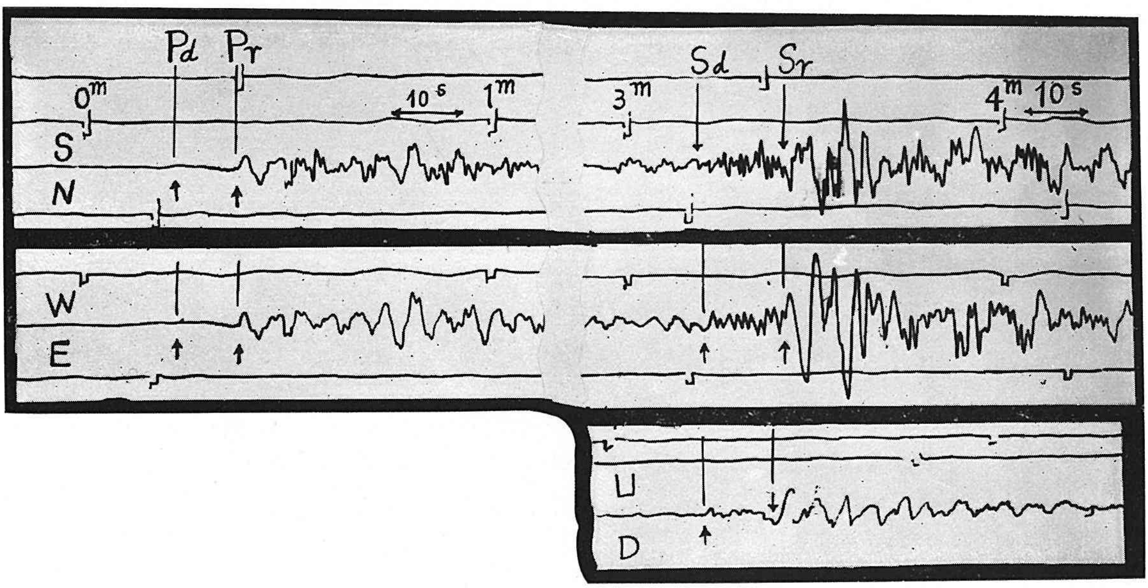

Fig. 2. (b) Fukushima (Δ=16.03°) The behaviours of *P*- and *S*-waves are the same as at Sendai.
(By the courtesy of the Fukushima Observatory)

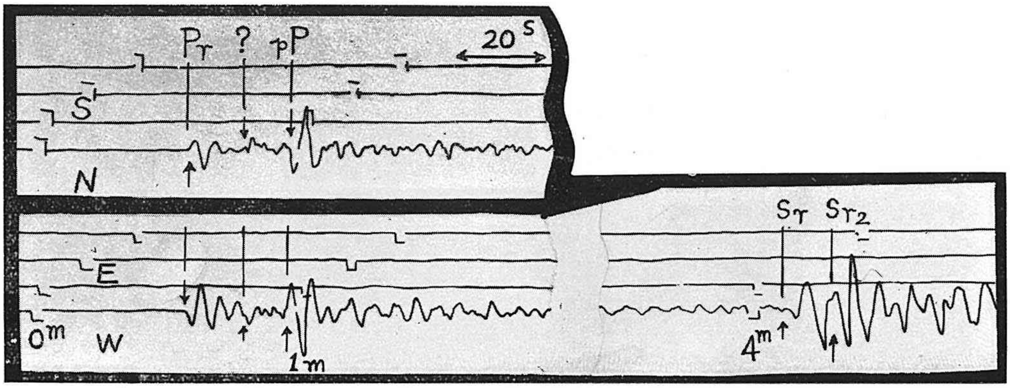

Fig. 2. (c) Gifu (Δ=19.73°) *Pr* and *Sr* appear as the first motion with the clear onset. (By the courtesy of the Gifu Observatory)

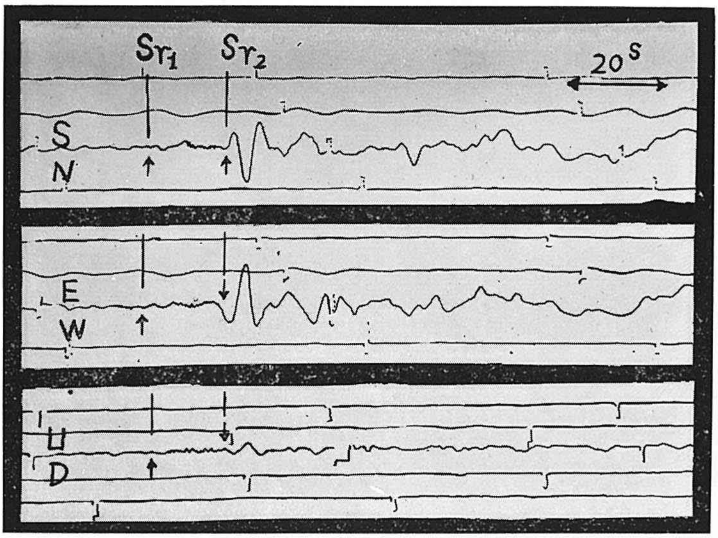

Fig. 7. Wiechert-seismograms, March 18th 00h 06m 46s, Near east coast of Kamchatka (referred to Table 6)

(a) Morioka (Δ=20.05°) A large Sr_2 arrives, forerun by a weak Sr_1.

(By the courtesy of the Morioka Observatory)

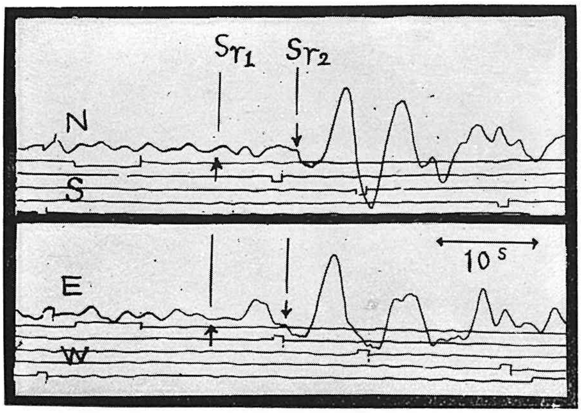

Fig. 7. (b) Sendai (Δ=21.35°) The behaviour of *S*-wave is the same as at Morioka.
(By the courtesy of the Sendai Observatory)

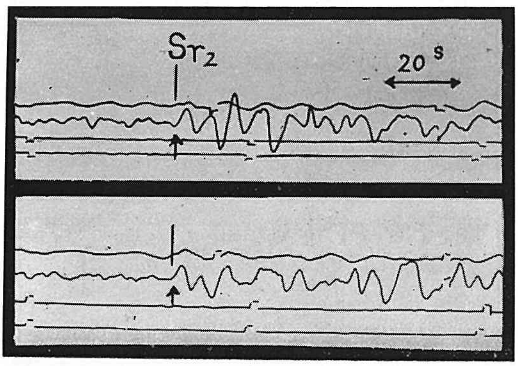

Fig. 7. (c) Shizuoka (Δ=25.21°) A clear Sr_2 appears as the first *S*-arrival.
(By the conrtesy of the Shizuoka Observatory)

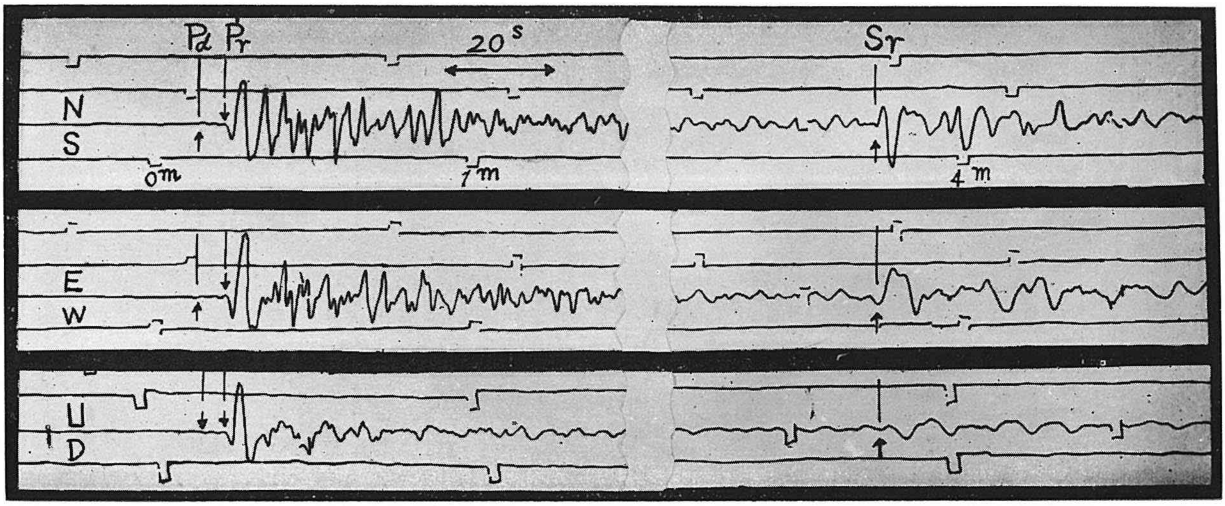

Fig. 12. Wiechert-seismograms, Aug. 22nd 06h 51m 37s, Near SE coast of Formosa (referred to Table 7)
(a) Kyoto (Δ=18. 00°) A weak *Pd* appears as the first *P*-motion, followed by a large *Pr*. As to *S*, the *Sd* being not observed, the *Sr* is only observed.
(By the courtesy of the Kyoto Observatory)

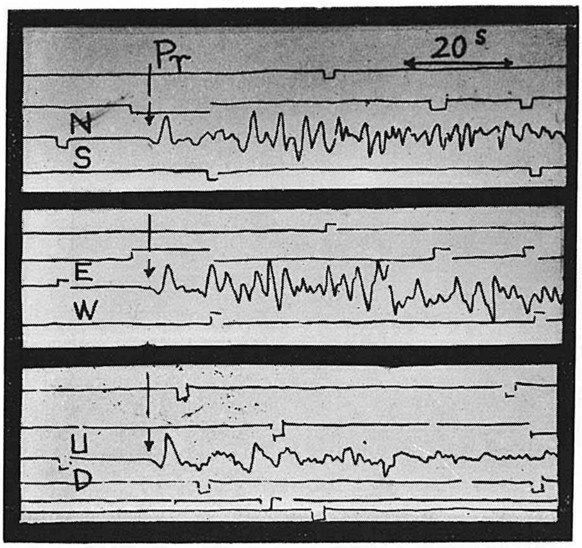

Fig. 12. (b) Sendai (Δ=23.27°) A clear *Pr* appears as the first motion.
(By the courtesy of the Sendai Observatory)